CHEMISTRY OF MATERIALS

Article

Improvement of Hydrogen Storage Properties of the Li–Mg–N–H System by Addition of LiBH

Jianjiang Hu, Yongfeng Liu, Guotao Wu, Zhitao Xiong, Yong Shen Chua, and Ping Chen

Chem. Mater., **2008**, 20 (13), 4398-4402• DOI: 10.1021/cm800584x • Publication Date (Web): 11 June 2008

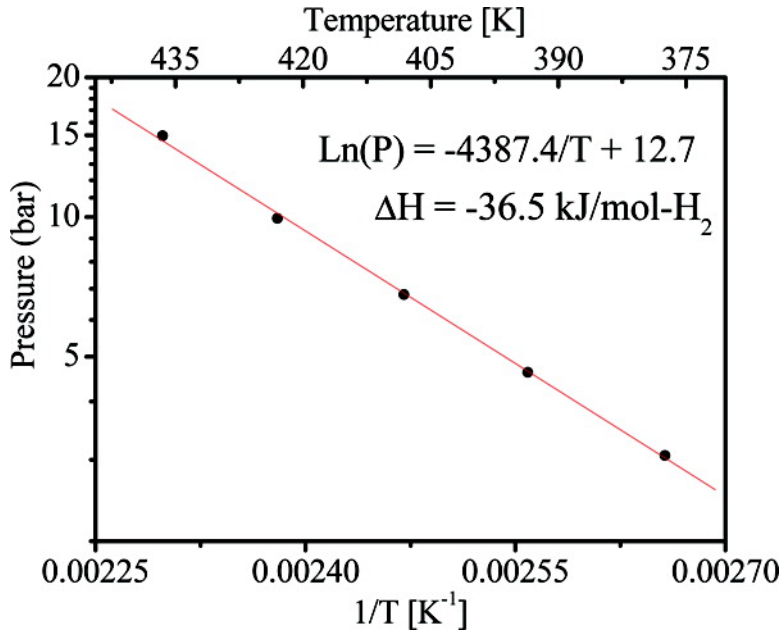

More About This Article

Additional resources and features associated with this article are available within the HTML version:

- Supporting Information
- Links to the 1 articles that cite this article, as of the time of this article download
- Access to high resolution figures
- Links to articles and content related to this article
- Copyright permission to reproduce figures and/or text from this article

View the Full Text HTML

Improvement of Hydrogen Storage Properties of the Li–Mg–N–H System by Addition of $LiBH_4$

Jianjiang Hu,[†] Yongfeng Liu,[†] Guotao Wu,[†] Zhitao Xiong,[†] Yong Shen Chua,[‡] and Ping Chen*[,†,‡]

Department of Physics, and Department of Chemistry, National University of Singapore, 10 Kent Ridge Crescent, Singapore 117543, Singapore

Received February 28, 2008. Revised Manuscript Received April 18, 2008

Significant improvements in the hydrogen desorption/absorption properties of the Li–Mg–N–H system have been achieved by adding a small amount of $LiBH_4$. The onset as well as the peak temperatures of hydrogen desorption shift to lower temperatures. Five wt % of hydrogen can be fully desorbed at 140 °C and reabsorbed at 100 °C. The kinetics of hydrogen desorption as well as absorption were found to be 3 times as fast as the pristine system. Thermodynamic analyses show that the temperature for equilibrium desorption pressure at 1 bar was 70 °C, which is about 20 °C lower than the pristine system. The enhancement in the hydrogen sorption properties was attributed to the weakening of N−H bonding in the metal amide molecules.

Introduction

Metal amide–hydride combined systems have been extensively investigated as materials for solid-state hydrogen storage since the discovery of the hydrogen storage in the $LiNH_2$–LiH system.[1] A variety of metal amide–hydride combinations have been investigated for their hydrogen sorption performances.[2–5] Investigations expand beyond the binary metal hydrides to metal complex hydrides.[6,7] Among the studied systems, the Li–Mg–N–H system comprised of LiH and $Mg(NH_2)_2$ exhibits moderate operation temperatures, good reversibility, and a relatively high capacity of 5.6 wt % and is therefore regarded as a promising candidate for on-board application.[2,3,8] Thermodynamic studies further indicate that this system can attain an equilibrium hydrogen pressure of 1 bar at ca. 90 °C,[8] which is close to the practical condition for PEM fuel cells. However, a rather high kinetic barrier has been identified in the hydrogen desorption from the system.[8,9] Kinetic improvements need to be made to obtain better hydrogen uptake/desorption properties to qualify this system to be a feasible hydrogen storage medium.

While some efforts have been invested in the compositional adjustment of LiH and $Mg(NH_2)_2$ to achieve high hydrogen capacities, others concern the understanding of hydrogen sorption mechanisms.[9–11] In contrast, attempts in the catalytic modification aiming at improving kinetics are sparse. Recently, Sudik et al. reported that kinetics was enhanced by seeding the desorption product, that is, $Li_2Mg(NH)_2$, which lowered the activation energy of desorption.[12] Starting with a ternary mixture $2LiNH_2 + LiBH_4 + MgH_2$, Yang et al. identified the reaction:

$$Mg(NH_2)_2 + 2LiH \text{---} Li_2Mg(NH)_2 + 2H_2 \quad (1)$$

during hydrogen desorption,[13] which was observed by Luo previously.[14]

$$2LiNH_2 + MgH_2 \rightarrow Li_2Mg(NH)_2 + 2H_2 \leftrightarrow Mg(NH_2)_2 + 2LiH \quad (2)$$

They found that $LiNH_2$ and $LiBH_4$ in the mixture first formed a quaternary hydride, which reacted with MgH_2. The resulted $Li_2Mg(NH)_2$ functioned as seeds that could reportedly enhance the hydrogen desorption reaction via the above reaction. Although more than 8 wt % of hydrogen could be released from the ternary mixture, the reversible part was about 2.5 wt %. Later, optimization was made by Lewis et al. by applying the combinatorial synthesis and screening (CSS) techniques on the ternary mixture system.[15] The optimum composition was found to be $0.6LiNH_2-0.3MgH_2-0.1LiBH_4$ with a reversibility of about 3.5 wt %.

* Corresponding author. Phone: +65 65165100. Fax: +65 67776126. E-mail: phychenp@nus.edu.sg.
[†] Department of Physics.
[‡] Department of Chemistry.

(1) Chen, P.; Xiong, Z. T.; Luo, J. Z.; Lin, J. Y.; Tan, K. L. *Nature* **2002**, *420*, 302–304.
(2) Xiong, Z. T.; Wu, G. T.; Hu, H. J.; Chen, P. *Adv. Mater.* **2004**, *16*, 1522–1525.
(3) Luo, W. *J. Alloys Compd.* **2004**, *381*, 284–287.
(4) Xiong, Z. T.; Hu, J. J.; Wu, G. T.; Chen, P. *J. Alloys Compd.* **2005**, *395*, 209–212.
(5) Hu, J. J.; Xiong, Z. T.; Wu, G. T.; Chen, P.; Murata, K.; Sakata, K. *J. Power Sources* **2006**, *159*, 116–119.
(6) Kojima, Y.; Matsumoto, M.; Kawai, Y.; Haga, T.; Ohba, N.; Miwa, K.; Towata, S. I.; Nakamori, Y.; Orimo, S. *J. Phys. Chem. B* **2006**, *110*, 9632–9636.
(7) Xiong, Z. T.; Wu, G. T.; Hu, J. J.; Chen, P. *J. Power Sources* **2006**, *159*, 167–170.
(8) Xiong, Z. T.; Hu, J. J.; Wu, G. T.; Chen, P.; Luo, W. F.; Gross, K.; Wang, J. *J. Alloys Compd.* **2005**, *398*, 235–239.
(9) Chen, P.; Xiong, Z. T.; Yang, L. F.; Wu, G. T.; Luo, W. F. *J. Phys. Chem. B* **2006**, *110*, 14221–14225.
(10) Leng, H. Y.; Ichikawa, T.; Hino, S.; Nakagawa, T.; Fujii, H. *J. Phys. Chem. B* **2005**, *109*, 10744–10748.
(11) Luo, W.; Stewart, K. *J. Alloys Compd.* **2007**, *440*, 357–361.
(12) Sudik, A.; Yang, J.; Halliday, D.; Wolverton, C. *J. Phys. Chem. C* **2007**, *111*, 6568–6573.
(13) Yang, J.; Sudik, A.; Siegel, D. J.; Halliday, D.; Drews, A.; Carter, R. O., III; Wolverton, C.; Lewis, G. J.; Sachtler, J. W. A.; Low, J. J.; Faheem, S. A.; Lesch, D. A.; Ozolins, V. *J. Alloys Compd.* **2007**, *446*, 345–349.
(14) Luo, W.; Rönnebro, E. *J. Alloys Compd.* **2005**, *404*, 392–395.

10.1021/cm800584x CCC: $40.75
Published on Web 06/11/2008

Table 1. Hydrogen Release during Ball Milling Treatment

$Mg(NH_2)_2$–LiH–$LiBH_4$	pressure increase (bar)	hydrogen released in ball milling step (wt %)
1−2−0	0.61	0.56
1−2−0.05	0.54	0.50
1−2−0.1	0.20	0.19
1−2−0.2	0.07	0.06
1−2−0.3	0.07	0.06

The ternary mixture $2LiNH_2 + LiBH_4 + MgH_2$ as hydrogen storage materials was found very recently by Yang et al. to be a self-catalyzed reaction.[16]

In our group, we have reported the effects of ionic hydride NaH and amide $NaNH_2$ on the kinetics of the system.[17] In this study, small amounts of the complex hydride $LiBH_4$ were added to the $Mg(NH_2)_2$–LiH (1:2) system to enhance the kinetics of hydrogen sorption of the $Mg(NH_2)_2$–LiH system.

Experimental Section

Sample Preparation. $Mg(NH_2)_2$ (>95%, synthesized in-house), LiH (95%, Sigma-Aldrich), and $LiBH_4$ (95%, Sigma-Aldrich) were loaded into a milling vessel in a glovebox with Ar as protecting atmosphere. Ball milling was conducted on a Retzsch PM400E at 200 rpm for 36 h. Molar ratios of $Mg(NH_2)_2$–LiH–$LiBH_4$ were 1−2−0.05, 1−2−0.1, 1−2−0.2, and 1−2−0.3, respectively. A sample of $Mg(NH_2)_2$–LiH at 1:2 molar ratio without $LiBH_4$ was also prepared as reference under the same milling conditions. Hydrogen release in the milling process was detected in terms of pressure increase in the milling vessels after ball milling. Table 1 lists the amount of hydrogen released during the ball milling process.

It was noticed that the pressure increase during ball milling was lower with more $LiBH_4$ addition, implying that the presence of $LiBH_4$ retards the hydrogen release in the ball milling process.

Methods. Temperature-programmed desorption (TPD) tests were carried out on a home-built apparatus, which was coupled with a mass spectrometer (MS) from Hiden Analytical, England, for the monitoring of NH_3 generation during dehydrogenation. The heating rate was 2 °C/min. Details about the apparatus have been described elsewhere.[18] The volumetric sorption measurements were performed on a commercial Sieverts' automatic gas reaction system from Advanced-Materials Corp., U.S. The hydrogen desorption isotherms were conducted at 140 °C for the comparison of desorption kinetics. The temperature of the gas reactor was raised to 140 °C from room temperature within 10 min and kept at this temperature for the whole period of measurement. Measurements of Fourier transform infrared spectroscopy (FTIR) were conducted on a Perkin Elemer FTIR-3000 unit in diffuse reflectance infrared Fourier transform (DRIFT) mode. The powdery samples were loaded into the DRIFT in situ cell in the glovebox and measured at a resolution of 4 cm^{-1}. For the X-ray diffractometry (XRD) measurements (Bruker D8-advance X-ray diffractometer with Cu Kα radiation), about 50−70 mg of sample was pressed into pellets and fixed to the XRD sample holder, which was housed inside a protective hood operating under vacuum. Differential scanning calorimetry (DSC) measurements were performed on a Netsch DSC 204 HP housed inside the glovebox. Samples were heated at 2 °C/min under the flow of purified Ar at 30 mL/min. Magic-angle-spinning solid ^{11}B nuclear magnetic resonance (NMR) experiments were carried out at room temperature on a Bruker Advance 400 NMR spectrometer operating at 9.7 T on 128.3 MHz ^{11}B frequency with $BF_3 \cdot Et_2O$ as reference. The measurement of the hydrogen pressure at equilibrium was conducted manually on a homemade apparatus equipped with a furnace and a pressure gauge. The temperature of the furnace was controlled with a resolution of 0.1 °C. A thermal couple was inserted into the sample to ensure the precision of sample temperature reading. The sample loading was about 2 g. The temperature was raised at 2 °C/min to the desired value and kept so long that the pressure reading remained unchanged for 2 days. The sample was then rehydrogenated at 110 °C and 70 bar for 25 h and cooled to room temperature within 10 h for the next measurement.

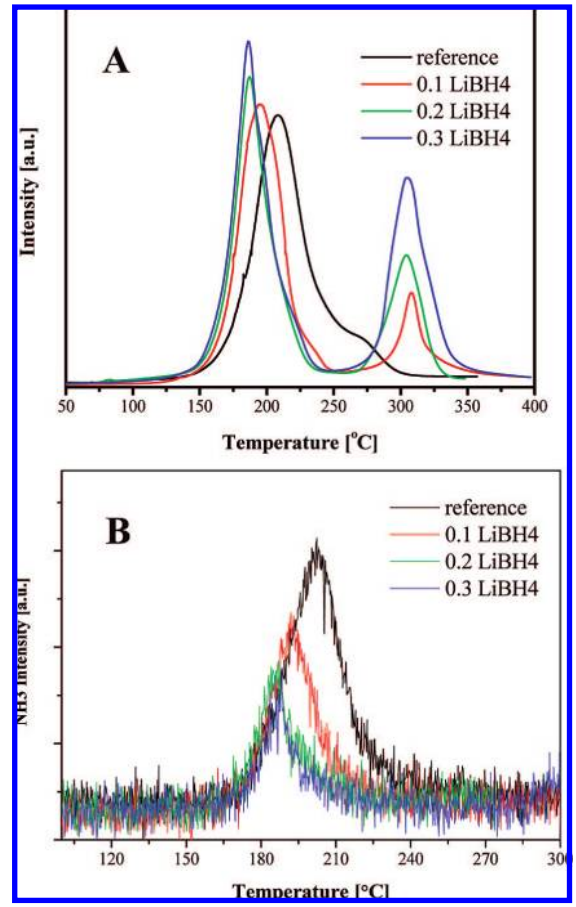

Figure 1. (A) TPD results of as-milled samples with $LiBH_4$ addition and (B) MS monitoring of NH_3 generation during dehydrogenation. The black line relates to the pristine sample.

Results and Discussion

Hydrogen Sorption Properties. The temperature-programmed desorption measurements show that the peak temperatures of hydrogen release are lower with the addition of $LiBH_4$ than the reference sample (Figure 1A). The desorption peaks are narrower than the pristine sample as well. However, with increased amount of $LiBH_4$, the hydrogen released in higher temperature range becomes more prominent, which may lead to mitigation of hydrogen

(15) Lewis, G. J.; Sachtler, J. W. A.; Low, J. J.; Lesch, D. A.; Faheem, S. A.; Dosek, P. M.; Knight, L. M.; Halloran, L.; Jensen, C. M.; Yang, J.; Sudik, A.; Siegel, D. J.; Wolverton, C.; Ozolins, V.; Zhang, S. *J. Alloys Compd.* **2007**, *446*, 355–359.
(16) Yang, J.; Sudik, A.; Siegel, D. J.; Halliday, D.; Drews, A.; Carter, R. O., III; Wolverton, C.; Lewis, G. J.; Sachtler, J. W. A.; Low, J. J.; Faheem, S. A.; Lesch, D. A.; Ozolins, V. *Angew. Chem., Int. Ed.* **2008**, *47*, 882–887.
(17) Liu, Y. F.; Hu, J. J.; Xiong, Z. T.; Wu, G. T.; Chen, P. *J. Mater. Res.* **2007**, *22*, 1339–1345.
(18) Chen, P.; Xiong, Z. T.; Luo, J. Z.; Lin, J. Y.; Tan, K. L. *J. Phys. Chem. B* **2003**, *107*, 10967–10970.

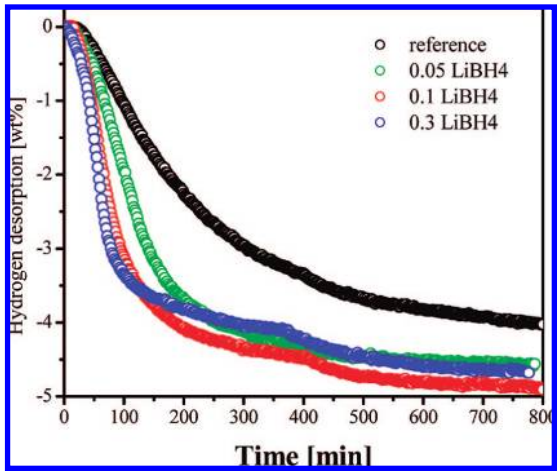

Figure 2. Isothermal hydrogen desorption at 140 °C of samples with various $LiBH_4$ concentrations.

deliverability in the lower temperature range. Simultaneous monitoring of NH_3 generation by the mass spectrometer indicates that NH_3 evolution was reduced with the addition of $LiBH_4$ (Figure 1B).

To evaluate the effects of $LiBH_4$ concentration, hydrogen desorption isotherms were measured (Figure 2). It can be seen that there is a dependence of the enhancement in the kinetics on the concentration of $LiBH_4$. As compared to the pristine system, a faster desorption kinetics can be achieved with 5 mol % addition of $LiBH_4$ (sample $Mg(NH_2)_2$–LiH–$LiBH_4$ 1−2−0.05). Doubling the amount of $LiBH_4$ further improves the kinetics. However, increase in the $LiBH_4$ amount to 30 mol % (sample $Mg(NH_2)_2$–LiH–$LiBH_4$ 1−2−0.3) only results in a slight enhancement in the kinetics. The small changes in slope at about 400 min were caused by the instrument between two sections of measurement.

The addition of $LiBH_4$ accounts for about 3% and 9% weight of the samples $Mg(NH_2)_2$–LiH–$LiBH_4$ 1−2−0.1 and $Mg(NH_2)_2$–LiH–$LiBH_4$ 1−2−0.3, respectively, which correspond to theoretical hydrogen capacities of 5.43 and 5.10 wt %, respectively. This is reflected in the desorption isotherms in Figure 2. However, there is a considerable amount of hydrogen released in high temperature range for the sample $Mg(NH_2)_2$–LiH–$LiBH_4$ 1−2−0.3 (Figure 1A), which seems inconsistent with the results measured in the isotherms. As reported in ref 16, the second part of hydrogen could be released according to the reaction between the ternary imide $Li_2MgN_2H_2$ and $LiBH_4$ as follows:

$$3Li_2MgN_2H_2 + 2LiBH_4 \longrightarrow 2Li_3BN_2 + Mg_3N_2 + 2LiH + 6H_2 \quad (3)$$

Because the amount of $LiBH_4$ used in this study was stoichiometrically less than $Li_2MgN_2H_2$ (0.667) in the above reaction, hydrogen release in this step should be proportional to the $LiBH_4$ amount following the above reaction, which is verified by the TPD observations in Figure 1A. Therefore, the decrease of hydrogen capacity in the lower temperature range is only correlated to the weight percentage of $LiBH_4$ addition. With 3−9 wt % of $LiBH_4$ added in this study, the hydrogen capacity in low temperature range is theoretically 5.43 and 5.10 wt %.

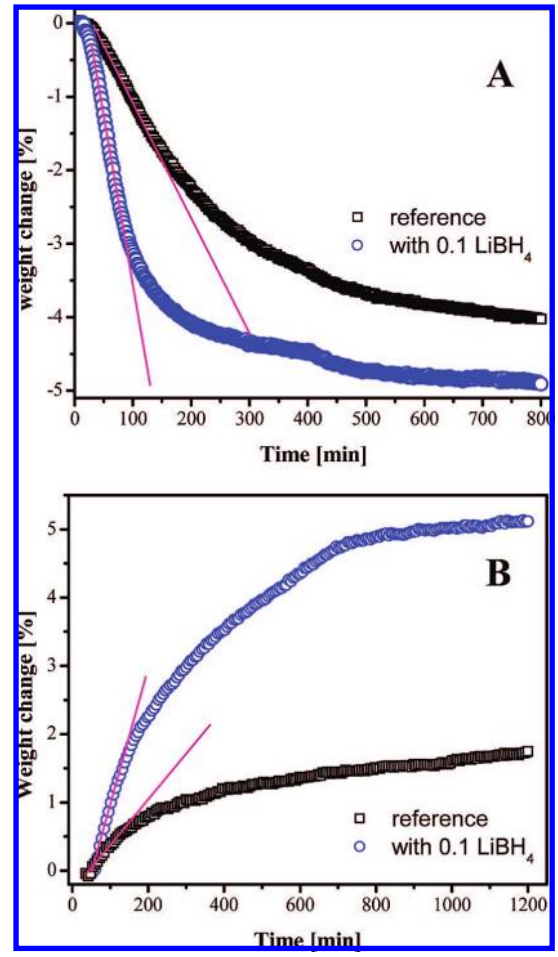

Figure 3. (A) Isothermal hydrogen desorption at 140 °C and (B) subsequent isothermal absorption at 100 °C and 78 bar (□ reference sample, ○ sample with 0.1 $LiBH_4$ addition).

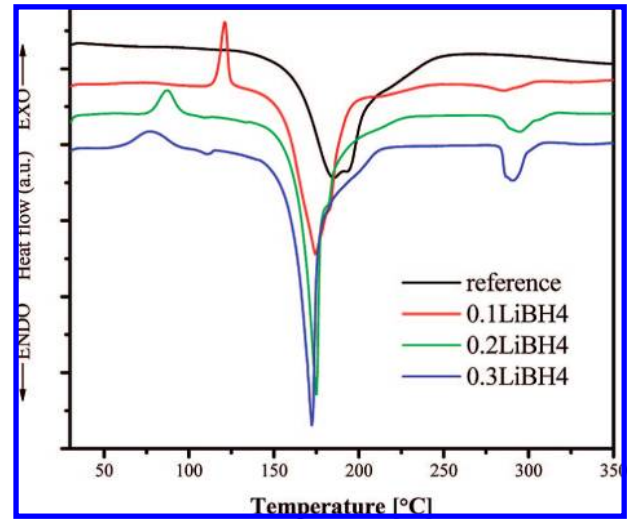

Figure 4. DSC results of as-milled samples with various concentration of $LiBH_4$.

The hydrogen desorption of the Li–Mg–N–H system follows a zero-order reaction kinetics for the initial stage, as a good linearity of the conversion against time was observed.[9] Shown in Figure 3A are the desorption isotherms at 140 °C. The sample with 10 mol % $LiBH_4$ (sample $Mg(NH_2)_2$–LiH–$LiBH_4$ 1−2−0.1) desorbs hydrogen up to 5 wt %, whereas only 4 wt % of hydrogen can be desorbed

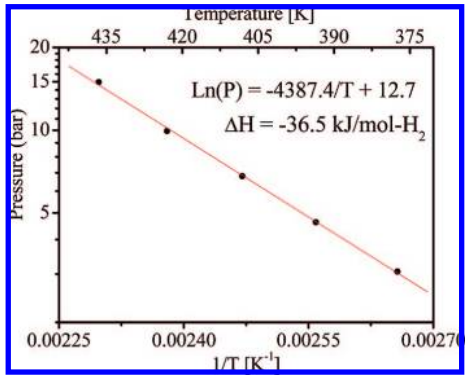

Figure 5. van't Hoff plot of the sample $Mg(NH_2)_2$–LiH–$LiBH_4$ 1−2−0.1.

from the sample without $LiBH_4$ addition. Analyzing the tangent slope of the linear parts for hydrogen desorption, the rate constant for the sample with $LiBH_4$ was estimated to be 0.046 wt % min^{-1}, about 3 times that without $LiBH_4$ (0.016 wt % min^{-1}). In the hydrogen uptake step (Figure 3B), the same sample with $LiBH_4$ also exhibits better performances over the reference sample. At the hydrogen pressure of ca. 78 bar and 100 °C, hydrogen uptake reaches 5 wt %, that is, fully recharged to the sample. The reference sample, in contrast, can only absorb 1.75 wt % hydrogen under the same conditions. Using the same approach, the rate constant of the hydrogen absorption for the sample with $LiBH_4$ was determined to be 0.020 wt % min^{-1}, again about 3 times that of the reference sample at the initial stage of absorption (0.007 wt % min^{-1}). Taking into account the purities of the starting materials, the introduction of $LiBH_4$ into the system did not lower the hydrogen deliverability.

Thermodynamic Properties. DSC measurements of the as-milled samples show a decrease in peak temperatures of hydrogen desorption at about 175 °C (Figure 4), consistent with the TPD tests. With increased amount of $LiBH_4$, the peak position shifts to lower temperature. The endothermic heat effects of the doped samples are comparable to those of the pristine sample. An additional exothermic event appears in the temperature range of 80−150 °C before the major endothermic dehydrogenation peak. The shape and heat effect of this exothermic peak obviously relates to the amount of $LiBH_4$ added to the system. With higher amount of $LiBH_4$, the exothermic change occurs at lower temperature. Corresponding to the hydrogen desorption in the high temperature range (Figure 1A), there is an endothermic peak at about 300 °C. The heat effect is obviously proportional to the $LiBH_4$ amount added. In contrast, the characteristic endothermic event of $LiBH_4$ crystal transition at about 120 °C was not detected. These observations may indicate the interaction of $LiBH_4$ with other components.

The equilibrium hydrogen desorption pressures at different temperatures in the range of 100−170 °C were measured for the sample with 10 mol % $LiBH_4$ (Figure 5). By linear fitting of the data, the dehydrogenation enthalpy was obtained to be 36.5 kJ/mol-H_2. This is a decrease by 2.4 kJ/mol-H_2 as compared to our previous report for the system without addition of $LiBH_4$,[8] indicating a possible change in the thermodynamic property. Extrapolating the line to 1 bar equilibrium pressure results in the temperature of 70 °C,

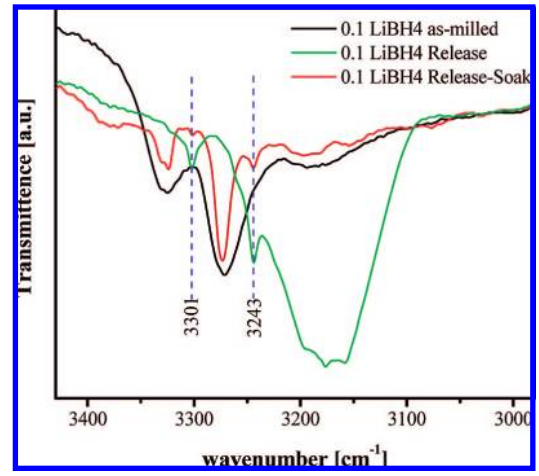

Figure 6. FTIR spectra of sample $Mg(NH_2)_2$–LiH–$LiBH_4$ 1−2−0.1.

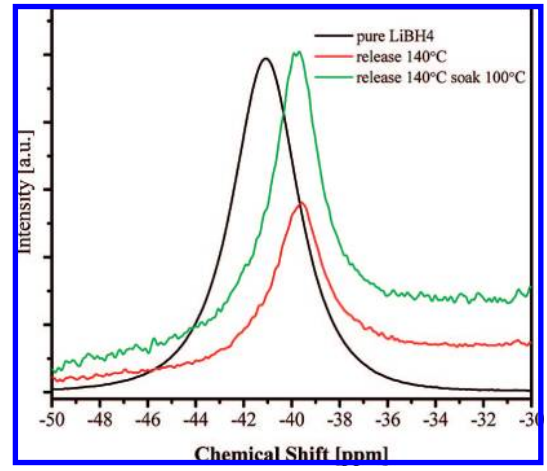

Figure 7. Solid ^{11}B NMR spectrum of the sample $Mg(NH_2)_2$–LiH–$LiBH_4$ 1−2−0.1 with different treatment.

which is 20 °C lower than that of the pristine sample, which is a step closer toward the on-board application. In fact, we can see from Figure 5 the equilibrium hydrogen pressure at 100 °C has become measurable with addition of $LiBH_4$. The value at 103 °C was measured to be 3.06 bar, an adequate parameter required by the proton exchange membrane (PEM) fuel cell operation. It should be noted that other researchers have reported equilibrium pressures at certain temperatures and there were some differences among values of the equilibrium pressure.[3,14,19–21]

Structural Analyses. The exothermic peak prior to the major endothermic event detected in the DSC measurements may infer the interactions of $LiBH_4$ with other components in the system. The as-milled sample shows the signature N−H vibration of $Mg(NH_2)_2$ at 3326/3272 cm^{-1} in the FTIR spectrum (Figure 6, black). However, besides the broad absorbance of the ternary imide $Li_2MgN_2H_2$ at about 3174 cm^{-1}, the FTIR spectrum of the dehydrogenated sample ($Mg(NH_2)_2$–LiH–$LiBH_4$ 1−2−0.1) shows two sharp peaks at 3243 and 3301 cm^{-1}, which did not originate from the starting compounds and persist after hydrogen desorption and

(19) Ichikawa, T.; Tokoyoda, K.; Leng, H.; Fujii, H. *J. Alloys Compd.* **2005**, *400*, 245–248.
(20) Aoki, M.; Noritake, T.; Nakamori, Y.; Towata, S.; Orimo, S. *J. Alloys Compd.* **2007**, *446*, 328–331.
(21) Janot, R.; Eymery, J. B.; Tarascon, J. M. *J. Power Sources* **2007**, *164*, 496–502.

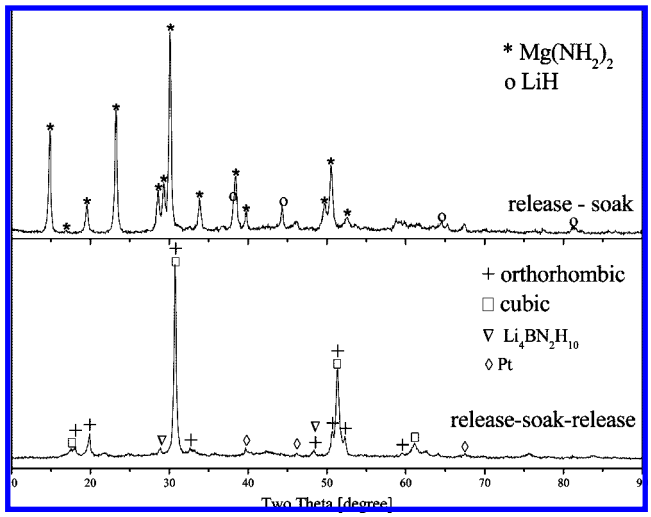

Figure 8. The XRD patterns of the sample $Mg(NH_2)_2$–LiH–$LiBH_4$ 1−2−0.1. Top: after dehydrogenation–rehydrogenation. Bottom: after dehydrogenation–rehydrogenation–dehydrogenation.

absorption (Figure 6). These new absorbances at 3243 and 3301 cm^{-1} were also reported by Chater et al. in a study on the reaction of $LiNH_2$ with $LiBH_4$.[22] They found that the two reactants formed a solid solution $(LiNH_2)_x(LiBH_4)_{(1-x)}$ and assigned the absorbances to the N−H bonds of $LiNH_2$ units in the solid solution. The shifting of N−H stretching from 3312/3258 cm^{-1} of pristine $LiNH_2$ to the lower wavenumbers at 3301/3243 cm^{-1} indicates a weakening of the N−H bonds. Pinkerton et al. found that a quaternary hydride with the composition of $Li_3BN_2H_8$ was readily formed from $LiNH_2$ and $LiBH_4$ at 2:1 molar ratio either spontaneously during ball milling or by heating the mixture of the two compounds below 100 °C.[23,24] The follow-up XRD analysis on the single crystal found its true composition was $Li_4BN_3H_{10}$. The N−H bond in the quaternary hydride was measured to be 0.84 Å, which is 10–20% longer as compared to 0.70−0.76 Å in $LiNH_2$,[25] another evidence of N−H weakening. Our previous studies on the mechanism of the Li–Mg–N–H system demonstrate that $LiNH_2$ is formed upon the dehydrogenation from $Mg(NH_2)_2$ and LiH.[26] The cationic transformation from $Mg(NH_2)_2$ + 2LiH to $2LiNH_2$ + MgH_2 in reaction 2 provides another possibility of $LiNH_2$ generation.[3,11] Therefore, we assume that $LiBH_4$ added to the system may have reacted in the exothermic event with the in situ formed $LiNH_2$, forming a product akin to the solid solution or the quaternary hydride.

However, no apparent changes were detected by FTIR measurements (not shown) in the region between 2000 and 2400 cm^{-1} concerning the B−H vibration for the samples undergone hydrogen sorption tests, implying that the tetrahedral structure of BH_4^- anions introduced as $LiBH_4$ remains intact, agreeing with the observation in ref 22. Nevertheless, detailed XRD examination showed that the B−H bonds in $(LiNH_2)_x(LiBH_4)_{(1-x)}$ were shorter than those in $LiBH_4$,[22] indicating a strengthening of the B−H bonds. While the solid-state ^{11}B NMR spectrum of $LiBH_4$ shows a single central transition at −41 ppm, the resonance of ^{11}B after dehydrogenation and rehydrogenation treatments was shifted to about −39 ppm (Figure 7), indicating a lower electron cloud density around B atom. One of the possible reasons for the subtle downfield shift of the ^{11}B resonance in the samples as compared to that in $LiBH_4$ (−41 ppm) may be the shortening of B−H bonds. Because H atom is more electronegative than B atom, electron cloud may be more biased to H atom when B atom is closer to H atom. Whether the coexisting amide anions NH_2^- of $LiNH_2$ in the vicinity of the BH_4^- anions also have influences on the chemical environment of B atom is unknown at the moment.

The seeding effects of $Li_2MgN_2H_2$ reported in ref 12 on enhancement of the hydrogen sorption kinetics may not apply in this case, as hydrogen evolution was suppressed in the ball milling step with the addition of $LiBH_4$ (Table 1). Thus, the formation of $Li_2MgN_2H_2$ as seeding species is not likely. The dehydrogenation from amide–hydride pairs inevitably involves the splitting of the N−H bond of amide anions. With weaker N−H bonds in the $(LiNH_2)_x(LiBH_4)_{(1-x)}$ solution, the dehydrogenation might take the pathway such that the N−H splitting could take place at the weakened N−H bonding in the $(LiNH_2)_x(LiBH_4)_{(1-x)}$ solution where the splitting would require less energy. The participation of $(LiNH_2)_x(LiBH_4)_{(1-x)}$ in the interface reactions of hydrogen desorption and absorption in the Li–Mg–N–H system may somehow experience reduced kinetic barriers, leading to faster kinetics. In-depth understanding on this interesting phenomenon deserves further investigation.

An orthorhombic structure is usually observed by XRD for the dehydrogenated $Mg(NH_2)_2$–LiH at 1:2 molar ratio.[26] However, the XRD profile of the sample added with $LiBH_4$ turned out to be a mixture of the orthorhombic and cubic structure after dehydrogenation (Figure 8). While no $LiBH_4$ diffraction was observed, the diffraction at 2θ 28.9° and 48.3° could be originated from the phase of $Li_3BN_2H_8$ or $(LiNH_2)_x$-$(LiBH_4)_{(1-x)}$, whose existence was observed clearly by the FTIR measurement. Pt diffraction was originated from the Pt sample holder.

Conclusions

Kinetic and thermodynamic improvements in the hydrogen sorption properties of the Li–Mg–N–H system were achieved by introducing a small amount of $LiBH_4$. With a small amount of $LiBH_4$, the kinetics of hydrogen release at 140 °C and uptake at 100 °C was accelerated by 2 times, while the temperature for equilibrium pressure at 1 bar decreases by 20 to 70 °C. The in situ formed solid solution from $LiBH_4$ and $LiNH_2$ with weakened N−H bonds may be attributed to the enhancement of the hydrogen sorption performances.

Acknowledgment. We are thankful for financial support from General Motors (U.S.) and the Agency for Science, Technology, and Research (A*Star) (Singapore).

CM800584X

(22) Chater, P. A.; David, W. I. F.; Johnson, S. R.; Edwards, P. P.; Anderson, P. A. *Chem. Commun.* **2006**, 2439–2441.
(23) Pinkerton, F. E.; Meisner, G. P.; Meyer, M. S.; Balogh, M. P.; Kundrat, M. D. *J. Phys. Chem. B* **2005**, *109*, 6–8.
(24) Meisner, G. P.; Scullin, M. L.; Balogh, M. P.; Pinkerton, F. E.; Meyer, M. S. *J. Phys. Chem. B* **2006**, *110*, 4186–4192.
(25) Filinchuk, Y. E.; Yvon, K.; Meisner, G. P.; Pinkerton, F. E.; Balogh, M. P. *Inorg. Chem.* **2006**, *45*, 1433–1435.
(26) Hu, J. J.; Liu, Y. F.; Wu, G. T.; Xiong, Z. T.; Chen, P. *J. Phys. Chem. C* **2007**, *111*, 18439–18443.